NONLINEAR C-SCAN ACOUSTIC MICROSCOPE AND ITS APPLICATION TO CHARACTERIZATION OF DIFFUSION- BONDED INTERFACES OF DIFFERENT METALS

K. Kawashima[1], M. Murase[1], Y. Ohara[1], R. Yamada[2], H. Horio[2], T. Miya[3] and F. Fijita[3]
[1] Nagoya Institute of Technology, Nagoya, Japan, [2] Daido Steel Co., Nagoya, Japan,
[3] SONIX K. K., Tokyo, Japan

Abstract: A nonlinear C-scan acoustic microscope for industrial application has been developed to image the second harmonic amplitude excited at semi-closed microcracks, kissing bonds, or bonded interfaces of different materials, which are impossible by the conventional C-scan acoustic microscope. The second harmonic images have high spatial resolution compared with the conventional C-scan images. The contrast of the second harmonic images is confirmed by FFT analysis of the received waveforms.

Introduction: The conventional C-scan acoustic microscope is useful for imaging of internal voids and cracks of finite volumes. However, imaging of semi-closed cracks and kissing bonds is very difficult due to partial transmission of ultrasonic waves across the closed cracks or gaps.

Nonlinear ultrasonic technique, in particular the measurement of the second harmonic amplitude, has been used for evaluation of dislocation density[1], fatigue cracks[2], precipitations[3], adhesive joint[4], sintered steel powder[5] and diffusion bonded interfaces[6,7]. Incident wave of finite amplitude, about ten times greater than the wave amplitude used for the conventional ultrasonic testing, can excite the second harmonic in solid materials by dislocation movement, nonlinear stress-strain response in compressive or tensile phase at bonded surface, clapping of closed crack surfaces. The second harmonic amplitude generated in metals by these mechanism is an order of 0.1~1% of the fundamental, incident, wave amplitude, therefore, piezo elements of a particular resonance frequency have been bonded to measure the second harmonic wave amplitude. Recently, the development of digital signal acquisition and signal processing make possible the second harmonic measurement with the conventional piezo transducers pressed on samples tested. This direct contact measurement, however, is not extended to image the second harmonic amplitude due to difficulty in scanning.

Several pioneering works on the second harmonic imaging have been reported[8,9,10] for nondestructive characterization of bonded parts. To obtain the second harmonic images of bonded areas in water immersion, the reduction or separation of strong acoustic nonlinearity of water is very important. The second harmonic generated in water could mask the variation of the second harmonic of bonded interfaces.

In the present paper, an approach to reduce the nonlinear effect of water is proposed. A nonlinear C-scan acoustic microscope of reflection as well as transmission mode is built. With the nonlinear acoustic microscope, we have visualized the second harmonic amplitude of diffusion- bonded interfaces of different metals.

Basic theory: Assume that a nonlinear elastic stress strain relation shown in Fig.1 is given by.

$$\sigma = K_2\varepsilon - K_3\varepsilon^2/2 \qquad (1)$$

The corresponding solution of wave equation is expressed by

$$u = U\exp i(kx-\omega t) + ((3K_2+K_3)/(8K_2))U^2\exp(2i(kx-\omega t)) \qquad (2)$$

where U is the fundamental wave amplitude, K_2 and K_3 are elastic stiffness of the second and third order, $\beta=(3+K_3/K_2)$ is the nonlinear parameter of the second harmonic. Equation (2) tells us that the second harmonic amplitude is proportional to the square of the fundamental wave amplitude and wave number as well as the propagation distance and β. When we use a burst wave of a fixed frequency, the second harmonic amplitude divided by U, the second harmonic ratio, is proportional to U, β and x.

For an elastic solid including planar gaps comparable to the incident wave amplitude, plane longitudinal wave will close the gap surfaces when the gap is smaller than the incident wave amplitude, as shown in Fig.2. In gap free area, the stress-strain relationship will be linear as shown in Fig.2 (a). In a gap of which opening is

smaller than incident wave amplitude, tensile stress will not be transmitted, while compression stress will be transmitted after closing the crack in compression phase as shown in Fig.2 (b and c). In gap area which opening is larger than ultrasonic amplitude, ultrasonic wave will not be transmitted as shown in Fig.2 (d). Thus, the stress-strain response passing through micro gaps is expressed by superposition of stress-strain relations shown in Fig. 2 (e). The elastic modulus is higher in compression than in tension, therefore, elastic wave propagates at higher velocity in compressive phase as shown in Fig.3 and, considering this waveform distortion in frequency domain, higher harmonics appear as shown in Fig.4. Thus, the clapping brings in marked nonlinearity in the transmitted wave as that of acoustic nonlinearity of nonlinear continuum.

It should be noted that the stress-strain relation shown in Fig.2 is extremely simplified. Namely, the real gaps or cracks have rough surface of the grain size order, therefore, the gap or crack surfaces will contact at some

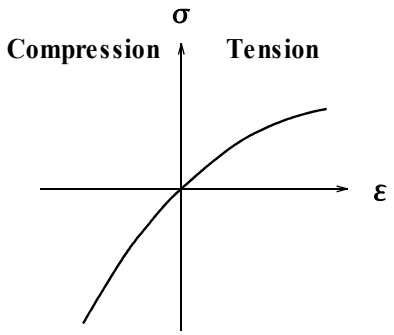

Fig. 1 Nonlinear elastic stress-strain curve.

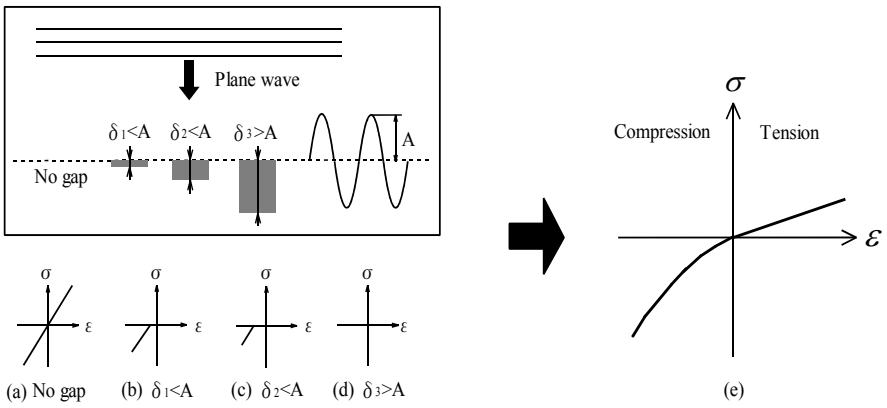

Fig. 2 Stress-strain response around minute gaps comparable to incident wave amplitude.

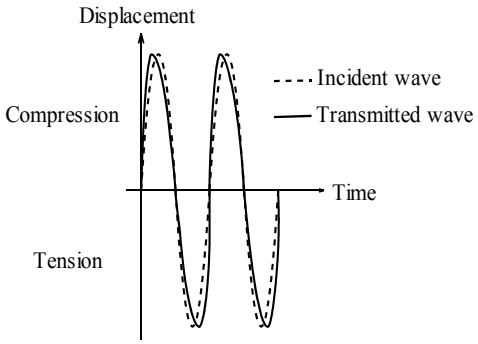

Fig.3 Waveform distortion.

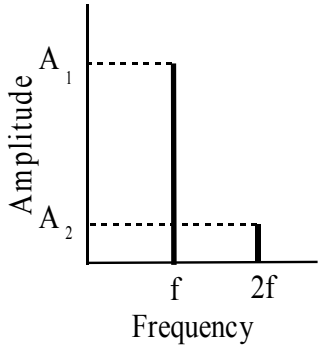

Fig.4 Generation of second harmonics.

points at first. Under compressive stress, the contact points extend to microscopic contact areas with local plastic deformation. Also, the plastic deformation accompanies hysteresis loop under crack clapping.

Experimental procedure: A schematic diagram of the nonlinear C-scan acoustic microscope is shown in Fig. 5. A conventional C-scan imaging system is extended to excite a tone-burst pulser and to extract the second harmonic components. Tunable analog bandpass filters are used to reduce the fundamental frequency component.

In water immersion test, the acoustic nonlinearity of water is generally much higher than that of the solid materials tested. The second harmonic amplitude of water increases as a quadratic function of the incident wave amplitude as well as incident frequency. To minimize the second harmonic of water, we should use lower fundamental frequency and incident wave amplitude. This, however, brings in low spatial resolution and weak second harmonic generation in samples. Depending on required spatial resolution and the expected amplitude of the second harmonic generated in samples, we should select appropriate frequency and amplitude of incident wave. Also, tuning of bandpass filters is important.

To demonstrate the effectiveness of the second harmonic imaging, we applied the nonlinear C-san acoustic microscope to examination of diffusion bonded[11] interfaces. Between steel and gamma titanium aluminide bars, Ni-based amorphous film was inserted. The bonding temperature was chosen lower than the melting point of base metal and higher than that of amorphous film. Bonding time is quite short, about 1 min., compared to

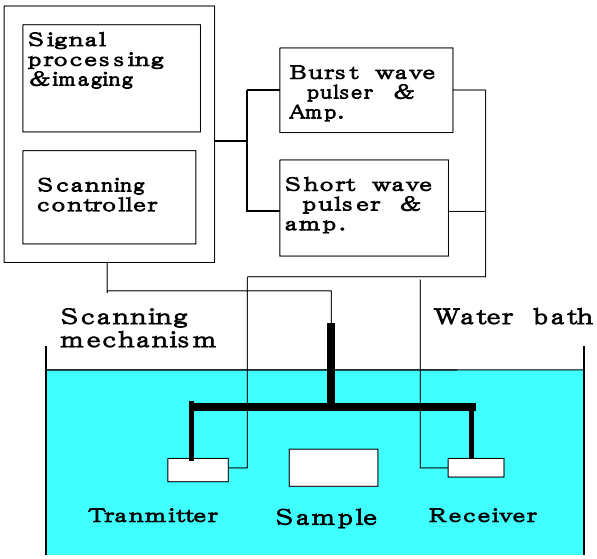

Fig. 5 Schematic diagram of a nonlinear C-scan acoutic microscope.

diffusion bonding because the amorphous film aids the diffusion for bond. Shielding gas is Argon to protect the generation of oxide film on bonding surface. Compressive stress of several MPa is applied to both bars, and only bonding part is heated by induction coil to minimize the heat influence of base metal. The samples are cylinders of 15 mm in diameter and 18 mm in length.

Experimental results and discussion: In the following, we show the conventional C-san image and the second harmonic images captured by reflection mode. A 5 MHz transducer of 1/4" in diameter and focal length of 2" was used for linear and nonlinear C-scan imaging. For the second harmonic imaging, we used bandpass filters to reduce the fundamental 3.5MHz component by 40dB.

Figures 6 and 7 show the image of the same bonded interface at the identical gate position. Compared with the conventional C-scan image shown Fig. 6, the second harmonic image in Fig. 7 gives high spatial resolution. At present, the reason of the image contrast is not clear, however, there may be some variation in filler components and distribution of minute gaps at diffusion bonded interface. To confirm the validity of the second

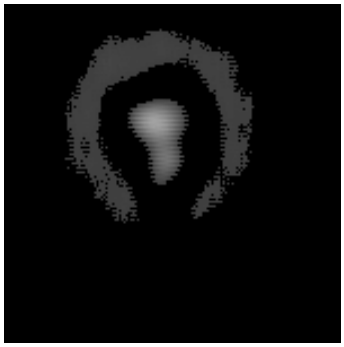

Fig. 6 Linear C-scan image.

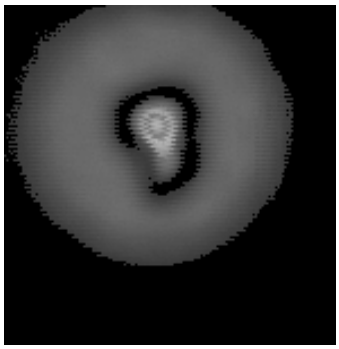

Fig. 7 The second harmonic Image.

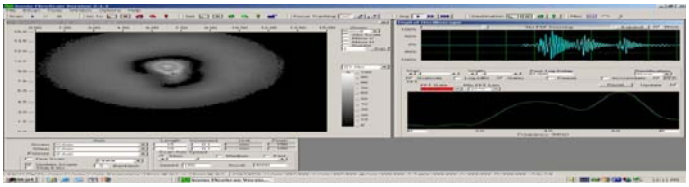

Fig. 10 Waveform and spectrum at point 3.

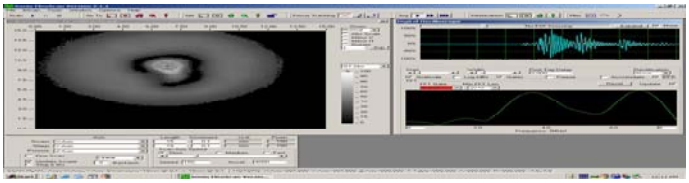

Fig. 11 Waveform and spectrum at point 4.

harmonic image, we captured time domain signals and their amplitude spectra at various positions, as shown in Figs. 8 to 11. The white + denotes the position where time domain signal was captured. In Fig.8, + is located in the brightest point, the lowest part in the bright ring.

The right upper widow shows the received signals, in which 7MHz component is amplified by 40 dB. The red horizontal line denotes the gate interval. In Figs. 8 and 9, the signal from the bonded interface is much higher than those in Figs. 10 and 11. The amplitude spectrum in lower right window shows large amplitude at 7 MHz in Figs. 8 and 9, but does comparable amplitude in 3.5 and 7 MHz in Figs. 10 and 11. These amplitude spectra prove that the second harmonic images are valid.

Conclusions: A nonlinear C-scan acoustic microscope has developed to visualize the distribution of the second harmonic amplitude. By selecting appropriate incident frequency and wave amplitude as well as tuning bandpass filters, we obtain the second harmonic images of high resolution. The validity of the harmonic images is confirmed by amplitude spectra at various positions.

Acknowledgement: This research has partly been supported by Grant in Aids for Scientific Research from Japanese Ministry of Education, Science and Culture (B 10450047, B 12555024) and Cooperative Research Grant from SONIX K.K. and Daido Steel Co.

References:

1. A. Hikata, B. B. Chick, and C. Elbaum, Appl. Phys. Lett., 3, 195(1963)
2. O. Buck, W. L. Morris, and J. M. Richardson, Appl. Phys. Lett., 3371, (1978).
3. J. H. Cantrell and W.T. Yost, Philos. Mag. A 69, 315 (1994).
4. M. Rothenfusser, M.Mayr and J. Baumann, Ultrasonics, 38, 322 (2000).
5. Y. Ohara, K. Kawashima, M. Murase, N. Hirose, Review of Progress in QNDE, eds. D. O. Thompson and D. E. Chimenti, 22B, 1257 (2003).
6. D. J. Barnard, G. E. Dace, D. K. Rehbein, and O. Buck, J. NDE, 16-2, 77(1997).
7. Y. Ohara, K. Kawashima, R. Yamada and H. Horio, Review of Progress in QNDE, eds. D. O. Thompson and D. E. Chimenti, 23B, in press (2004).
8. T. P. Berndt and R. E. Green Jr., Nondestructive Characterization of Materials IX, 394 (1999).
9. F. M. Severin, B. O'nail and R. Maev, Review of Progress in QNDE, eds. D. O. Thompson and D. E. Chimenti, 19A, 881(2000).
10. C. Mattei and P. Marty, Review of Progress in QNDE, eds. D. O. Thompson and D. E. Chimenti, 23A, 989 (2003).
11. T.Shimizu, H.Horio, J. Japan Weld. Soc., 66-6, 14(1997).